Divergent assemblage patterns of abundant and rare microbial sub-communities in response to inorganic carbon stresses in a simultaneous anammox and denitrification (SAD) system

Duntao Shu, Hong Yue, Yanling He, Gehong Wei

PII: S0960-8524(18)30308-0
DOI: https://doi.org/10.1016/j.biortech.2018.02.111
Reference: BITE 19621

To appear in: *Bioresource Technology*

Received Date: 17 January 2018
Revised Date: 20 February 2018
Accepted Date: 22 February 2018

Please cite this article as: Shu, D., Yue, H., He, Y., Wei, G., Divergent assemblage patterns of abundant and rare microbial sub-communities in response to inorganic carbon stresses in a simultaneous anammox and denitrification (SAD) system, *Bioresource Technology* (2018), doi: https://doi.org/10.1016/j.biortech.2018.02.111

Divergent assemblage patterns of abundant and rare microbial sub-communities in response to inorganic carbon stresses in a simultaneous anammox and denitrification (SAD) system

Duntao Shu[a], Hong Yue[b], Yanling He[c], Gehong Wei[a] *

[a] State Key Laboratory of Crop Stress Biology in Arid Areas, College of Life Sciences, Northwest A&F University, Yangling, Shaanxi 712100, China

[b] State Key Laboratory of Crop Stress Biology in Arid Areas, College of Agronomy and Yangling Branch of China Wheat Improvement Center, Northwest A&F University, Yangling, Shaanxi 712100, China

[c] School of Human Settlements & Civil Engineering, Xi'an Jiaotong University, Shaanxi 710049, China

Abstract

Inorganic carbon has profound influence on anammox system and distinct microbial communities play pivotal roles in nitrogen removal, yet little is known about the ecological patterns of abundant and rare sub-communities in response to inorganic carbon stresses in simultaneous anammox and denitrification systems. Here the aspects of community ecology of abundant and rare taxa under abiotic constraints were explored. Results showed that different IC/NH_4^+-N ratios have significant influences on NH_4^+-N and TN removal. Co-occurrence networks revealed that abundant and rare taxa present contrasting assemblage patterns and ecological strategies. Spearman's

* Corresponding author. Email: weigehong@nwsuaf.edu.cn.

correlation indicated that environmental filtering had discrepancy influences on these two bacterial sub-communities. Moreover, rare taxa were the key regulators for NH_4^+-N accumulation and NO_2^--N consumption. qPCR results indicated that nitrogen removal was mediated by multiple nitrogen transformation pathways. These findings collectively suggest that abundant and rare sub-communities have discrepant ecological patterns and provide insights into their structure-functional relationships.

Keywords: Rare sub-community; IC/NH_4^+-N ratio; Anammox; Functional gene; Ecological association

1. Introduction

In recent decades, biological nitrogen removal processes is in a period of significant change motivated by the following two aspects. On the one hand, there is a need to renew some wastewater treatment plants that was built in the last 30 years. On the other hand, the drive from the increasingly stringent effluent nutrient guidelines are being implemented across the world (Lettinga, 2014). Hence, there is major need for energy neutrality and resource recovery in industrial and municipal wastewater treatment plants (WWTPs). Anaerobic Ammonium oxidizing (anammox)-based processes have already been running successfully in many engineered WWTPs (Kartal et al., 2013; Ma et al., 2017), given their cost-effective and energy-efficient in terms of nitrogen removal. Of these processes, simultaneous anammox and denitrification (SAD) processes have evolved as a strategy to address energy autarky, N_2O emission and carbon footprints. However, the sensitivity of anammox bacteria to environmental variables, including pH,

dissolved oxygen (DO), and C/N ratio, among others, have been limiting factors for the side-stream and main-stream applications of SAD processes (Du et al., 2014; Ge et al., 2018; Li et al., 2016). Previous literature reported that inorganic carbon has been widely considered to be an important factor in single anammox processes (Jin et al., 2014; Kimura et al., 2011), nitritation-anammox processes (Ma et al., 2015), and completely autotrophic nitrogen removal over nitrite (CANON) processes (Zhang et al., 2016). In terms of SAD processes, anammox and denitrification simultaneously occur in one single reactor, with anammox bacteria and denitrifiers as functional genera. Since inorganic carbon serves as the bicarbonate alkalinity and an assimilation carbon source for these functional microorganisms, there is no doubt that inorganic carbon concentration is a pivotal factor affecting SAD process. Additionally, from a practical perspective, previous studies have shown that the inorganic levels in municipal wastewater streams with IC/NH_4^+-N ratio (0.1:1 to 4:1) can significantly affect nitrogen-cycling-related bacteria (Ma et al., 2015; Zhang et al., 2016). Thus, the influent concentration of inorganic carbon is crucial for SAD process and be worthy to investigated.

Microbial aggregates are unique microbial ecosystems and play key roles in SAD processes. The microbial communities are composed of a few highly abundant species and a large proportion of rare species. Abundant microorganisms account for the majority of bacterial biomass and element cycling in most ecosystem. Rare species with low abundance, termed “rare sub-communities,” which may help maintain ecosystem

stability and function (Lawson et al., 2015; Liu et al., 2015). Over the last decade, with the rapid development of high through-put sequencing, many multi-omic investigations have provided considerable insight into the bacterial assembly and temporal dynamics of SAD systems (Ge et al., 2018; Li et al., 2016). Although these studies effectively link whole bacterial community compositions to treatment performance in SAD system, they neither account for the assembly of abundant taxa and rare taxa nor determine the dynamics of these bacterial sub-communities in relation to IC/NH_4^+-N stresses in SAD process. Studies assessing the ecological patterns of abundant and rare sub-communities in SAD systems remain scarce. There is only one study that has been conducted in the activated sludge bioreactor, and this study illustrated that the rare taxa were more dynamics than the general taxa (Kim et al., 2013). Thus, whether abundant microorganisms present contrasting biodiversity patterns or discrepant underlying community assembly mechanisms compared with rare taxa in response to IC/NH_4^+-N stresses in SAD process remains unclear.

SAD processes are mediated by several nitrogen-cyling-related genes, such as anammox 16S rRNA, archaea ammonia monoooxygenase (*AOA amoA*), ammonia monoooxygenase (*AOB amoA*), nitrite oxidoreductase (*nxrA*), periplasmic nitrate reductase (*napA*), membrane-bound nitrate reductase (*narG*), dissimilatory nitrate reductase (*nrfA*), copper-containing nitrite reductase (*nirK*), nitrite reductase (*nirS*), and nitrous oxide reductase (*nosZ*). Although the ecological association between these functional gene fragments have been well established in wetland and denitrification

biofilters (Zhi et al., 2015), little is known about the effect of IC/NH_4^+-N ratios on the dynamics of their associated functional genera in SAD processes. Knowledge on the assemblage of functional genera and the links to the different IC/NH_4^+-N ratio constraints is not only essential for the robust implementation of SAD processes under fluctuating of influential conditions, but will also be useful for understanding the ecological patterns of abundant and rare taxa under abiotic stresses.

Given the above arguments, the present study was performed with the following objectives: (1) Do abundant and rare taxa present contrasting patterns under different IC/NH_4^+-N ratio stresses? (2) What are the co-occurrence of abundant and rare sub-communities? And what are the major drivers that influenced the dynamics of abundant and rare taxa? (3) Which bacterial sub-communities are the key regulators for nitrogen transformation?

2. Methods

2.1. Anammox biomass and long-term experimental procedures

The anammox biomass used in this study was collected from a laboratory-scale sequencing batch reactor (SBR) that has been operated for over four years. The operation temperature, hydraulic residence time (HRT), influent NH_4^+-N, and influent NO_2^--N were 32 ±2^oC, 4 h, 199±4.5 mg-N/L, and 221±5.6 mg-N/L, respectively. The long-term removal efficiencies of NH_4^+-N and NO_2^--N were maintained at 92±0.6 and 94±0.8%, respectively. According to the previous study (Shu et al., 2015), "*Ca. Brocadia sinica*" (accession number KP721346-KP721365) were the predominant

anammox bacteria in this SBR system.

For long-term experiments, ~1.2 L seeding sludge was taken from the above SBR system and were cultivated in a new SBR system with a working volume of 2.8 L. The SAD system was operated at 32±2^{o}C and 6 h cycles in a greenhouse following the previous study. In this study, the reactor was fed with distinct $KHCO_3$ to result in an IC to NH_4^+-N concentration ratio of 0~1.3. To maintain the stability of simultaneous anammox and denitrification, the mixed solution (5 g COD/L) of sodium acetate and propionate was added into the reactor automatically to result in an influent COD (chemical oxygen demand)/TN (total nitrogen) ratio of 0.31. In addition, the SAD system was fed with trace element solution and mineral medium containing 199±4.5 mg/L NH_4^+-N and 221±5.6 mg/L NO_2^--N.

2.2. DNA extraction, PCR amplification, Illumina MiSeq sequencing, and sequence processing

Prior to DNA extraction, the individual sludge samples were pooled from five specimens at the end of each phase in the SAD system. Then, 2.0 mL anammox biomass for each sample was used to extract genomic DNA by using FastDNA® SPIN Kit for Soil (Mp Biomedicals, Illkirch, France). The purified genomic DNA were then amplified by PCR using 338F and 806R primers for amplification of the hypervaribale V3-V4 region. Finally, the purified amplicons were sequenced on the Illumina MiSeq PE300 platform. The raw data is publicly available in NCBI SRA database under accession number SRR3566108.

2.3. Quantitative real-time PCR

The absolute abundance of bacterial 16S rRNA, anammox 16S rRNA, *AOA* amoA, *AOB* amoA, *nxrA*, *narG*, *napA*, *nrfA*, *nirS*, *nirK*, and *nosZ* genes in each sample were quantified by Mastercycler ep realplex (Eppendorf, Hamburg, Germany) based on the SYBR Green II method. The qPCR reaction was performed in 10 μL mixtures containing 5 μL SYBR® Premix Ex Taq™ II (Takara, Japan), 0.25 μL of each primer, 1 μL of genomic DNA and 3.5 μL dd H_2O. The primer pairs, standard plasmids, and qPCR protocols followed previous study (Shu et al., 2015). Triplicate reactions were conducted for each DNA sample.

2.4. Chemical and Statistical analyses

The influent and effluent samples were taken from the reactor on a daily basis. Then, samples were filtered through a 0.45 μm pore diameter membrane and were analyzed immediately. The concentrations of NH_4^+-N, NO_2^--N, and NO_3^--N were measured using a Lachat Quik Chem 8500 Flow Injection Analyzer (Lachat Instruments, Milwaukee, USA), and COD were analyzed using Hach TNT 830 reagent with a spectrophotometer (DR 2800, Hach, USA). The measurement of IC concentrations were carried out with the TOC analyzer (vario TOC cube, Elementar, Germany).

For statistical analyses, it was defined OTUs (operational taxonomic units) as "abundant" if their average relative abundances > 0.05% and "rare" when their abundances < 0.001%; those in between belong to transient taxa (Liu et al., 2015). *P*-values ($P< 0.05$) were considered significant and corrected for multiple testing using

a false discovery rate (FDR) of 5% (q< 0.05) with the q-value function performed in *BiocLite* R (https://bioconductor.org/biocLite.R) unless otherwise indicated. After sub-sampling and cumulative sum scaling (CSS) normalization of OTU matrices, α-diversities at a 97% similarity were measured using the Qiime platform (https://qiime.org). (Un)weighted UniFrac distance matrices were calculated to assess the discrepancies in bacterial communities (β-diversity). Nonmetric multidimensional scaling (NMDS) was performed to evaluate the similarity between samples. Principal coordinate analysis (PCoA) was performed to further assess differences in microbial communities.

Redundancy ordination analysis (RDA) was conducted to elucidate the influences of environmental parameters on OTUs affiliated with rare and abundant taxa. Spearman's rank correlation values between environmental parameters and relative abundances of OTUS were calculated, then the significantly Spearman's rank association values (both positive and negative) between OTUs and environmental parameters were visualized in Cytoscape (Ver 3.5.0, http://www.cytoscape.org). In addition, all possible pairwise Spearman's rank correlations between those OTUs associated with rare, abundant and transient sub-communities were calculated to explore their co-occurrence patterns. The co-occurrence networks were visualized using Gephi (Ver 0.9.1, https://gephi.org). Network-level and node-level topological properties were further calculated to compare the topology of the rare taxa sub-network with the abundant taxa sub-network.

Potential functional genera were blasted against the MiDAS database

(http://www.midasplatform.org). In addition, the functional gene prediction and metabolic pathway reconstruction were performed via Tax4Fun analysis (http://tax4fun.gobics.de) based on KEGG category. Finally, the quantitative response relationships between nitrogen transformation rates and functional gene fragments were determined via step regression models. Subsequently, direct and indirect effects of gene fragments on nitrogen transformation rate were calculated via path analysis. All above statistical analyses were performed in R with corresponding packages (Ver 3.4.1, R development core team 2014) unless otherwise indicated.

3. Results and discussion

3.1. Treatment performance of SAD system in response to different IC/NH_4^+-N ratio constraints

In this study, as shown in Fig. 1, experiments were conducted without addition of COD in phase I (1-20 days) to maintain the stability of autotrophic anammox system. During phase I, the observed NH_4^+-N, NO_2^--N, and total nitrogen removal (TN) efficiencies were 94.88±1.80%, 99.69±0.84%, and 90.64±0.84%, respectively. The average nitrogen stoichiometric ratios of $\Delta NO_2^-/\Delta NH_4^+$ and $\Delta NO_3^-/\Delta NH_4^+$ were 1.26±0.05 and 0.21±0.03, respectively, which were consistent with the theoretical ratios for anammox (Strous et al., 1999). During phase II (21-40 days), the experiments were carried out without the addition of inorganic carbon but with COD added, and the NH_4^+-N removal efficiencies plummeted to 80.42±1.51%. However, the NO_2^--N and TN removal efficiencies declined slightly to 97.15±0.21% and 85.51±0.73%, respectively.

The average nitrogen stoichiometric ratios of $\Delta NO_2^-/\Delta NH_4^+$ increased to 1.43±0.05, but $\Delta NO_3^-/\Delta NH_4^+$ declined to 0.11±0.03, respectively. One-Way ANOVA tests for phase I and II indicate that NH_4^+-N removal shows significant differences ($P< 0.05$) under different IC/NH_4^+-N ratios. In addition, when a lower concentration of COD was added in the reactor, the absence of inorganic carbon had no significant influence on NO_2^--N and TN removal.

During phases III, IV and V, with the increase of IC/NH_4^+-N ratios from 0.1 to 0.7, the NH_4^+-N, NO_2^--N, and TN removal efficiencies increased gradually to 90.59±0.85%, 99.36±0.09%, and 95.46±0.37%, respectively. The nitrogen loading rate (NLR) and nitrogen removal rate (NRR) also increased gradually (Fig. 1). In addition, the COD removal efficiencies increased from 34.05±2.30% (phase II) to 59.81±2.01% (phase V), indicating that the seeding of anammox sludge had adapted to new circumstances. Therefore, a IC/NH_4^+-N ratio of 0.7 was ideal this SAD process, which was inconsistent with previous studies, possibly because these experiments were performed on the single anammox reactor (Kimura et al., 2011) and nitritation-anammox reactor (Ma et al., 2015) rather than SAD processes. During phase VI (101-120 days), further increasing the ratio of IC/NH_4^+-N to 1.0 decreased the NH_4^+-N and TN removal efficiencies to 84.84±0.83% and 87.45±0.59%. Meanwhile, the accumulation of effluent NO_3^--N was observed (Fig. 1). This result indicated that the stability of the SAD system had been disturbed and anammox microorganisms were slightly suppressed in this phase. During phase VII (121-140 days), the amount of inorganic matter increased to a IC/NH_4^+-N ratio of 1.3.

As predicted, anammox was significantly inhibited, as revealed by the poor NH_4^+-N (76.95±1.33%) and TN (79.74±0.87%) removal efficiencies. However, although a sizable accumulation of effluent NH_4^+-N and NO_3^--N was observed, the NO_2^--N and COD removal efficiencies slightly decreased to 93.75±0.85% and 35.37±4.56%. It was therefore concluded that heterotrophic microorganisms, including nitrite-N denitrifying bacteria and acid-forming bacteria were one of the primary reasons accounted for this NO_2^--N removal (Du et al., 2014).

Over the course of the whole experiment, One-Way ANOVA tests illustrated that different IC/NH_4^+-N ratios had profound impacts on NH_4^+-N and TN removal ($P< 0.05$), while they had no significant effects on NO_2^--N removal ($P> 0.05$). This was partly consistent with previous study (Zhang et al., 2016), indicating that sufficient IC suppressed activity of anammox but removed the inhibition on nitrified oxidizing bacteria or nitrite-dependent denitrifiers. One possible reason explaining this downturn in anammox activity under high IC input is that when low IC is supplied, the added HCO_3^- acts as a carbon source for anammox microorganisms and heterotrophic denitrifiers. Therefore, the NH_4^+-N, NO_2^--N, and TN removal efficiencies gradually increased during phases II-V. With the increase of IC, the residual HCO_3^- could not be fully utilized by anammox. In the SAD process, H^+ was consumed by the anammox reaction while denitrification produced H^+. Therefore, surplus HCO_3^- and the produced H^+ resulted in an increased pH in the SAD system. Finally, the higher concentrations of free ammonia (FA) or free nitrous acid (FNA) contributed to the observed poor SAD

reactor performance (Jin et al., 2014). On the other hand, the sufficient IC input disrupted the ecological balance in the SAD system. Intra-association and Inter-association of species change with new conditions. Although the anammox bacteria was the dominant process in the SAD system, the roles of abundant and rare taxa in this reactor are worth to be investigating.

3.2. Heterogeneity of abundant and rare sub-community

In this study, after quality filtering and global trimming, a total of 149,108 bacterial 16S V3-V4 high-quality sequences with an average read length of 450 bp were generated for all sludge samples. In order to avoid sequencing bias, the dataset was randomly sub-sampled 100 times to yield 11,168 reads for each sample, which were then clustered into 2495 bacterial OTUs based on a 97% similarity threshold. To explore the *a*-diversity of these samples, Chao 1 estimates, Shannon-Wiener indices, and Simpson estimate were calculated. The rarefaction curves indicated that although the diversity of the whole community was covered in the present sequencing depth, rare species could only emerge with an increase of sequencing depth. In addition, results showed that community diversity indices (richness, diversity, and evenness) differed among these samples. Chao 1 estimate of the phase V was 1.1~1.2 fold higher than that of other phases. Shannon-Wiener indices and Simpson estimate in phase V were also 1.1~1.3 fold higher than that of other phases except phase I. These results demonstrated that although these samples were highly similar, phase V had higher community richness and evenness than the of other samples.

To explore the ecological patterns of rare and abundant sub-communities, the distribution of abundant, transient, and rare taxa among taxonomy levels (from phylum to genus) were further investigated. The abundant and rare taxa contained 116 and 822 OTUs, accounting for 4.6% and 32.9% of the total OTUs, respectively. The transient taxa were comprised of 1557 OTUs, accounting for 62.4% of the total OTUs. Additionally, the core taxa (245 OTUs, accounting for 9.8% of total OTUs) were further defined. To reveal the prevalence of the different bacterial sub-communities (abundant, rare, and transient taxa) in the core microorganisms (Astudillo Garcia et al., 2017), their proportions were calculated across the dataset. Interestingly, it was observed that the core taxa were dominated by abundant and transient taxa, accounting for 46.5% (114 OTUs) and 53.5% (131 OTUs) of core taxa. No of rare taxa belonged to the core sub-community, partially consistently with previous study (Jiao et al., 2017), indicating that rare and abundant taxa present contrasting patterns in the study.

From the perspective of community assembly and dynamics, the community composition of abundant, rare, and transient taxa differed substantially (Fig. 2). Results showed that abundant sub-communities across whole dataset were generally composed of 33.8% *Proteobacteria*, 33.9% *Chloroflexi*, and 8.8% *Planctomycetes* (Fig. 2a). *Proteobacteria* also accounted for a large proportion of phyla (49.1%) in the rare sub-community, followed by *Chloroflexi* and *Planctomycetes* at the relative abundances of 15.4% and 5.1% respectively (Fig. 2b). Additionally, it was observed that abundant taxa were shared by all samples, while rare taxa were only shared by samples from

phase IV, phase V, and phase VII. Compared with abundant and rare sub-communities by Wilcoxon Rank Sum tests, the results suggest that abundant and rare sub-communities have significant differences ($P< 0.05$) under IC/NH_4^+-N ratio constraints. In terms of transient taxa and whole communities (Fig. 2c, d), *Proteobacteria*, *Chloroflexi*, and *Planctomycetes* were also the dominant phyla in the SAD system, similar to the result of bacterial composition in the nitritation-anammox system (van Teeseling et al., 2015). These phyla may thus play pivotal roles for nitrogen removal. Within *Proteobacteria*, *α-Proteobacteria*, *β-Proteobacteria*, *γ-Proteobacteria*, and *δ-Proteobacteria* appeared in all samples in abundant and transient taxa, but only in phase IV, phase V and phase VII in rare taxa. *ε-Proteobacteria* only appeared in phase VII. These results suggest that different survival strategies had been adopted by abundant, rare, and transient taxa in response to IC stresses, although these shared phyla had some similarities between treatment phases.

3.3. Linkages between environmental variables and microbial communities

Based on the unweighted UniFrac distance matrices, results of PCoA revealed that the majority of the discrepancies between abundant and rare sub-communities could be attributed to different IC/NH_4^+-N ratios. The first two axes explained 57.4% and 51.9% of variance in the abundant sub-community and whole communities, which was higher than that of in the rare sub-community (44.2%). The results demonstrated that the rare sub-community had distinct biodiversity patterns compared to abundant taxa and whole communities. In addition, based on the weighted UniFrac distances, NMDS results

revealed that grouping patterns were strongly influenced by different IC/NH_4^+-N ratios. It was observed that samples from lower IC/NH_4^+-N ratios (0~0.4) and higher IC/NH_4^+-N ratios (0.7~1.3) clustered more closely in the abundant taxa and whole communities, respectively. The result of Mantel tests based on the Spearman's correlation (999 permutations) further confirmed that the abundant sub-community (R^2=0.832, P< 0.001) was more similar to the whole community than the rare sub-community (R^2=0.658, P< 0.001). Previous studies about community dynamics in natural ecosystems (i.e. lakes across China, the northwestern Pacific Ocean) reported that abundant and rare sub-communities had discrepant ecological niches (Liu et al., 2015; Wu et al., 2017). The similar results were observed in an activated sludge bioreactor (Kim et al., 2013). The present study corroborate those findings and provided further evidence in the SAD system to verify that rare sub-communities was not a random distributions of taxa. Given the NO_2^--N removal efficiency in phases IV-VII, it was therefore concluded that rare sub-communities had restricted distribution and contributed greatly to NO_2^--N removal.

Previous studies indicated that local environmental variables had influences on microbial communities in engineered WWTPs (Ju & Zhang, 2015; Luo et al., 2017; Shu et al., 2016), particularly for abundant and rare sub-communities in natural ecosystems (Liu et al., 2015). Results of RDA analysis in the present study indicated that the IC/NH_4^+-N ratio was a primarily factor in shaping the abundant sub-community. COD was the major driver shaping rare sub-community. In the transient sub-community, a

large proportion of genera were clearly related to the IC/NH_4^+-N ratio, effluent NO_3^--N, and NO_2^--N removal rate. Spearman's correlation network was further applied to explore the significant correlations between environmental attributes and assembly of bacterial sub-community (Fig. 3).

Generally, different environmental variables constrained the shaping of abundant and rare sub-community structures. Previous studies have demonstrated that *Candidatus Brocadia* and *Candidatus Jettenia* have the capacity to utilize organic matter in the organotrophic anammox process (Winkler et al., 2012). However, organic matter was limited in the whole phases (COD/TN=0.31) and it was first utilized by the dominant genus (e.g., *Ca. Brocadia*). It seems that *Ca. Brocadia* and *Ca. Jettenia* compete for nutrient resource (Feng et al., 2018) under IC/NH_4^+-N ratio stresses. Hence, the genus of *Ca. Jettenia* showed positive correlations with the IC/NH_4^+-N ratio and effluent NO_3^--N, but had negative correlations with the COD removal rate and TN removal rate. In contrast, *Ca. Brocadia* had positive correlation with COD removal rate and TN removal rate (Fig. 3a), indicating the inter-specific competition between *Ca. Brocadia* and *Ca. Jettenia* (Lawson et al., 2017). In the rare sub-community, *Ca. Brocadia* only had positive association with COD removal rate. We kept the COD/TN ratio at 0.31 to maintain the stability of the SAD process with *Ca. Brocadia* as the dominant anammox bacteria, although it was inhibited in the higher IC/NH_4^+-N ratios (0.7~1.3). It was therefore observed that *Ca. Brocadia* and *Kuenenia stuttgartiensis* showed a positive correlation with the TN removal rate in the transient sub-community. These results

indicated that abundant and rare bacteria have different ecological strategies, and environmental filtering had different influences on these two bacterial sub-communities.

3.3. Co-occurrence patterns of different bacterial sub-communities

In natural ecosystems, bacterial groups live together within complicated networks through mutualism, competition, and commensalism interactions (Deng et al., 2016). In the present study, the global network was constructed for whole community; the sub-networks were constructed from the OTUs affiliated with abundant, rare, and transient sub-communities. The global network contained 2,407 nodes (OTUs) and 209,551 edges. Of these nodes, 92, 823, and 1,492 belonged to abundant, rare and transient sub-networks. Topological features, including betweenness, closeness, node transitivity, and degree were calculated on the base of unique node-level (Fig. 4). As shown in Fig. 4a, the link of intra-associations between abundant and transient sub-communities was greater than that between transient and rare sub-communities. In addition, as shown in Fig. 4c and e, the value of betweenness and node transitivity in abundant sub-network was higher than that of rare sub-network, suggesting that abundant sub-communities were more widely distributed than rare sub-communities. Consistently, abundant sub-communities had wider niche breadths than rare sub-communities (Wu et al., 2017). Additionally, more negative correlations affliated with rare taxa (Fig. 3b) indicated that rare sub-communities had been faced strong negative selection from abiotic stresses due to their narrow niche breadths.

Notably, as shown in Fig. 4b, the entire global network could be parsed into six major

modules. Modules I and II account for 15.29% and 12.01% of the whole network. The values of closeness and degree in rare sub-network were higher than those in abundant and transient sub-networks, indicating that rare sub-communities had higher incidence of intra-taxon co-occurrence patterns.

To confirm the roles of abundant and rare sub-communities in the global network, the OTUs-related sub-networks were further generated. Compared to the Erdös–Réyni random network, these sub-networks (abundant, rare and transient) had higher modularity (MD), clustering coefficient (CC), average path length (APL), and network diameter (ND), indicating that abundant, rare and transient sub- communities had non-random co-occurrence patterns. The APL and CC index of 1.85 and 1.00 in sub-networks (abundant and rare) strongly indicated that the observed networks have“small world” properties. MD indices of 0.75 and 0.62 (> 0.4) in abundant and rare sub-networks revealed that these networks have modular structures (Deng et al., 2016). Furthermore, the average degree (AD) and graph density (GD) in rare sub-networks were higher than that in abundant sub-networks, confirming that rare sub-communities have a higher incidence of intra-associations. This result is inconsistent with previous study in oil-polluted soil (Jiao et al., 2017). Possible explanations are the discrepancy of dominant microorganisms in the corresponding ecosystem and different levels of environmental stresses.

Taken together, results showed that abundant and rare sub-communities displayed contrasting co-occurrence patterns, alluding to their different survival strategies under

abiotic stresses. For instance, the abundant taxa (i.e., *Ca.* Brocadia) prefers the *S*-strategy cope with the different IC/NH_4^+-N ratios, while the rare taxa (i.e., *Ca.* Kuenenia) adopted the *K*-strategy to face the higher IC stresses (> 0.7) (Kartal et al., 2013). Additionally, abundant taxa rarely co-occurred with rare taxa, while rare taxa often co-occurred with transient taxa. In view of these network-level topological features, the results revealed that rare sub-communities had more connections and closer intra-associations, although the abundant sub-community had a cosmopolitan distribution. Therefore, it is reasonable to conclude that rare taxa do indeed grow and play key roles for resilience of the SAD system under higher IC/NH_4^+-N stresses.

3.4. Functional genera and *key genes of nitrogen cycling*

Considering that the SAD performance is ultimately determined by the different functional bacteria, it is necessary to analyze the structure-functional relationship of abundant taxa and rare taxa. It should be noted that because the anammox-related genes (i.e., *Hzs* and *Hdh*) lacked good representative sequences in the KEGG database, the prediction of nitrogen pathway is limited. However, c-di-GMP, a key second messenger, plays pivotal roles in the aggregation of anammox in response to feeding loadings (Guo et al., 2017). Therefore, c-di-GMP was selected in the present study to explore the dynamics of anammox bacteria and we manually retrieved functional genes associated with nitrogen cycling from the KEGG database following previous study (Guo et al., 2016).

Since the anammox bacteria was the dominant microorganism in all phases, the

abundance of c-di-GMP in lower IC/NH_4^+-N ratios (0~0.4) exceeded that in higher IC/NH_4^+-N ratios (0.7~1.3). The *nasA* gene, associated with assimilatory nitrate reduction genes, was more abundant than *nasB* and *nirA* genes. As for denitrification genes, *nirK*, *nosZ*, *norC*, *qnorB*, *nirS*, and *nirD* were predicted to be more abundant in phase VII. All functional genes, including *narG*, *napA*, and *nrfA*, et. al., had higher predicted abundance in phases III-V. In addition, genes associated with ammonia oxidation (*amoB*/*C* and hao) had higher abundance in phase V-VII (Fig. 5a). KEGG category analysis showed that samples in phases III-VI (IC/NH_4^+-N ratios is 0.1~1.0) have more functional genes for the TCA cycle (1.01~1.35%) and nitrogen metabolism (2.60~2.84%). Notably, compared with other phases, samples from phase VII have more functional genes for fatty acid metabolism (0.057%), indicating that higher IC/NH_4^+-N promoted organic matter oxidation in these heterotrophic microorganisms. These results indicated that the coupling of anammox and denitrification was the primary reason accounted for nitrogen removal under higher IC/NH_4^+-N ratios (> 0.7)

To elucidate which bacterial taxa in abundant and rare sub-communities was responsible for the corresponding nitrogen conversion pathway, all assigned genera were further blasted with the MiDAS database (Fig. 5b, c). Of filtered genera, 11 and 12 functional genera were obtained for abundant and rare sub-communities, respectively. Functional genera, including *Ca. Brocadia*, *Nitrospira*, *Thauera*, et.al., were shared by abundant, rare and transient sub-communities (Fig. 5b, c), implying that these functional genera are generalists who plays pivotal roles for nitrogen and COD removal (Ju et al.,

2014; Shu et al., 2016). According to MiDAS, these functional genera were annotated as 8 functional groups, including AOB, nitrite oxidizing bacteria (NOB), anammox, heterotrophic microorganism (HET), phosphate accumulating organisms (PAO), glycogen accumulating organisms (GAO), nitrite-reduction bacteria (NIR), and nitrate-reduction bacteria (NAR). *Ca. Brocadia* (1.8~9.8%) and *Ca. Jettenia* (0.007~0.17%) were the dominant anammox bacteria in the abundant sub-community, while *Ca. Brocadia* (0~0.04%) was only annotated in the rare sub-community. The dynamics of anammox bacteria in the SAD system indicate that lower IC/NH_4^+-N ratios were beneficial to *Ca. Brocadia*, while *Ca. Jettenia* preferred to higher IC/NH_4^+-N ratios. Previous study revealed that *Ca. Jettenia* have the capable of oxidizing volatile fatty acid (Huang et al., 2014). Combined analysis of treatment performance of SAD system (Fig. 1) and Spearman's correlation results (Fig. 3) suggest that higher IC/NH_4^+-N ratios select for *Ca. Jettenia* and play a key role for the simultaneous removal of COD and nitrogen under abiotic stress conditions. Due to the limitation of sequencing depth, AOB (i.e., *Nitrosomonadace*) was only assigned on the family level, accounting for 0.1~0.7 % of total sequences. Similarly, *Nitrospira* appeared to use the *K*-strategy, classifying it as NOB, accounting for 0.01~0.4% and 0~0.03% of the abundant sub-community and rare sub-community, respectively. The abundance of AOB and NOB were higher in phases II-IV than that in phases V-VII (Fig. 5b, c). Functional genera associated with HET, including *Thauera*, *Dokdonella*, and *Amaricoccus*, were shared by abundant, rare and transient sub-communities (Fig. 5b, c). However, other

denitrifiers such as *Comamonas* and *Thermomonas* only appeared in transient sub-communities. NIR and NAR, typical of HET, were more abundant in phases VI-VII. Neither PAO nor GAO were annotated in the SAD system, except for *Propionivibrio* in rare taxa in phase VII. Taken together, higher IC/NH_4^+-N (> 0.7) was beneficial for HET, NIR, NAR, and *Candidatus Jtttenia*, while lower IC/NH_4^+-N (< 0.7) was favorable for AOB and NOB, indicating that ecological strategies are closely correlated with environmental filtering (i.e., IC/NH_4^+-N ratios) (Ju et al., 2014). Nevertheless, the molecular mechanism of these functional genera under abiotic stresses needs to be further investigated by employing metatranscriptomic and metaproteomics approaches base on RNA and protein levels.

3.5. Ecological associations and quantitative response relationships

To further corroborate the results from Tax4Fun and MiDAS, the absolute abundances of nitrogen functional genes were quantified (Fig. 6). During phases I-VII, the bacterial abundance remained in the same order of magnitude under different IC/NH_4^+-N ratio stresses (1.42×10^9-6.42×10^9copies/(g wet sludge)), indicating that the whole bacterial community is relatively stable under stresses. Similarly, the absolute abundances of anammox bacteria in phases I-VII were observed to be nearly the same order of magnitude (1.26×10^8-5.85×10^8copies/(g wet sludge)), revealing that the anammox biomass in this SAD system had a certain resistance to abiotic stresses (Zhang et al., 2017). Consistent with results of MiSeq sequencing, the anammox bacteria was the dominant functional genera for nitrogen removal.

The copy numbers of nitrification groups, including AOA *amoA*, AOB *amoA*, and *nxrA genes*, are summarized in Fig. 6. The abundances of AOA *amoA* and *nxrA* genes were not significantly different between phases, while the gene copies of AOB *amoA* varied significantly. Notably, the gene copies of *AOA amoA* and *nxrA* in phases V-VI were nearly one order of magnitude higher than that in phases II-IV and phase VII, which does not completely accord with Tax4Fun, probably due to the KEGG limitation. Nevertheless, these results are consistent with the results from Tax4Fun and MiDAS in that lower IC/NH_4^+-N ratio is beneficial for AOB. As for dissimilatory nitrogen reduction genes (i.e., *nrfA*, *napA*, and *narG*), their gene copy numbers in phases V-VI were nearly one to two orders of magnitude higher than that in phases II-IV and phase VII. These results confirm that appropriate IC/NH_4^+-N ratios (0.7-1.0) are favorable for denitrification and DNRA. Similar results were observed in three denitrification groups (i.e., *nirK*, *nirS*, and *nosZ*) and are in accordance with KEGG results.

Additionally, the quantitative response relationships between nitrogen transformation rates and nitrogen gene fragments were performed by stepwise regression models and path analysis. As a result, the NH_4^+-N transformation rate was collectively determined by *Anammox/AOA, Anammox/nrfA,* (*nirS+nirK+nrfA*)*/bacteria, and nrfA/nxrA* (Table S4) (P=0.032). The relative abundance ratios of these four gene fragments differed substantially under different IC/NH_4^+-N ratios. The variables *Anammox/AOA* and *Anammox/nrfA* were denoted as NH_4^+-N level consumption, while (*nirS+nirK+nrfA*)*/bacteria* and *nrfA/nxrA* in the equation denoted as NH_4^+-N

accumulation. Due to the relatively low abundance of AOA *amoA*, *nrfA* and *nxrA* genes, results from the path analysis showed that *Anammox/AOA* (-0.101) and *Anammox/nrfA* (0.031) had small direct effects on NH_4^+-N consumption, while (*nirS+nirK+nrfA*)*/bacteria* and *nrfA/nxrA* had higher direct effects on NH_4^+-N accumulation. Thus, anammox and DNRA were the key pathways for NH_4^+-N transformation. The accumulation of NH_4^+-N appeared in phases VI-VII along with higher IC/NH_4^+-N ratio, and these factors were favorable for *nrfA*- and *anammox*-related bacteria in rare sub-communities; this suggests that rare taxa are the key regulators for NH_4^+-N accumulation but that abundant taxa are responsible for NH_4^+-N consumption.

The transformation of NO_2^--N was jointly determined by *AOA/bacteria*, (*AOA+AOB)/(nxrA+anammox+nirS+nirK*), and *nirK/nxrA* (*P*=0.011). *AOA/bacteria* denoted as NO_2^--N accumulation; and (*AOA+AOB)/(nxrA+anammox+nirS+nirK*) and *nirK/nxrA* denoted as NO_2^--N consumption. Results indicated that simultaneous nitrification, anammox, and denitrification (SNAD) were responsible for NO_2^--N removal. It should be noted that dissolved oxygen was not strictly controlled in the present study and this is the potential reason that nitrification contributed to NO_2^--N removal. In addition, a higher direct effect of *nirK*/*nxrA* (0.609) was observed compared with (*AOA+AOB)/(nxrA+anammox+nirS+nirK*) (0.466). With respect to TN removal, (*narG+napA*)*/nxrA*, *narG/bacteria and nirK/Anammox* were the key factors for TN transformation (*P*=0.018). Direct effects of three gene fragments on TN transformation

further confirm that nitrogen removal in this SAD system was regulated by multiple nitrogen transformation pathways (Zhang et al., 2017).

4. Conclusion

Results elucidated that abundant and rare bacteria have discrepant assemblage patterns under IC/NH_4^+-N ratio stresses, and that environmental filtering has different influences on these two bacterial sub-communities. In addition, *Ca. Brocadia* were often the dominant species and had higher resistance to IC stresses. Higher IC/NH_4^+-N ratio (0.7~1.3) was beneficial for HET, NIR, NAR, and *Ca. Jettenia*, while lower IC/NH_4^+-N ratios (0~0.7) were favorable for AOB and NOB. Rare taxa were the key regulators for NH_4^+-N accumulation and NO_2^--N consumption. qPCR results corroborated that coupling of nitrification, anammox and denitrification accounted for nitrogen removal in this study.

Acknowledgement

This study was financially supported by National Science Foundation of China (41701291), China Postdoctoral Science Foundation (2017M620473), and Ph. D start-up fund of Northwest A&F University (Z109021641).

Appendix A. Supplementary data

E-supplementary data for this work can be found in e-version of this paper online.

References

1. Astudillo Garcia, C., Bell, J.J., Webster, N.S., Glasl, B., Jompa, J., Montoya, J.M., Taylor, M.W., 2017. Evaluating the core microbiota in complex communities: A

systematic investigation. Environ. Microbiol. 19(4), 1450-1462.

2. Deng, Y., Zhang, P., Qin, Y., Tu, Q., Yang, Y., He, Z., Schadt, C., Zhou, J., 2016. Network succession reveals the importance of competition in response to emulsified vegetable oil amendment for uranium bioremediation. Environ. Microbiol. 18(1), 205-218.
3. Du, R., Peng, Y., Cao, S., Wu, C., Weng, D., Wang, S., He, J., 2014. Advanced nitrogen removal with simultaneous Anammox and denitrification in sequencing batch reactor. Bioresour. Technol. 179, 497-504.
4. Feng, Y., Zhao, Y., Guo, Y., Liu, S., 2018. Microbial transcript and metabolome analysis uncover discrepant metabolic pathways in autotrophic and mixotrophic anammox consortia. Water Res. 128, 402-411.
5. Ge, C., Sun, N., Kang, Q., Ren, L., Ahmad, H.A., Ni, S., Wang, Z., 2018. Bacterial community evolutions driven by organic matter and powder activated carbon in simultaneous anammox and denitrification (SAD) process. Bioresour. Technol. 251, 13-21.
6. Guo, J., Peng, Y., Fan, L., Zhang, L., Ni, B., Kartal, B., Feng, X., Jetten, M.S., Yuan, Z., 2016. Metagenomic analysis of anammox communities in three different microbial aggregates. Environ. Microbiol. 18(9), 2979-2993.
7. Guo, Y., Liu, S., Tang, X., Wang, C., Niu, Z., Feng, Y., 2017. Insight into c-di-GMP Regulation in Anammox Aggregation in Response to Alternating Feed Loadings. Environ. Sci. Technol. 51(16), 9155-9164.

8. Huang, X., Gao, D., Tao, Y., Wang, X., 2014. C2/C3 fatty acid stress on anammox consortia dominated by "Candidatus Jettenia asiatica". Chem. Eng. J. 253, 402-407.
9. Jiao, S., Chen, W., Wei, G., 2017. Biogeography and ecological diversity patterns of rare and abundant bacteria in oil contaminated soils. Mol. Ecol. 26(19), 5305-5317.
10. Jin, R., Yu, J., Ma, C., Yang, G., Zhang, J., Chen, H., Zhang, Q., Ji, Y., Hu, B., 2014. Transient and long-term effects of bicarbonate on the ANAMMOX process. Appl. Microbiol. Biotechnol. 98(3), 1377-1388.
11. Ju, F., Xia, Y., Guo, F., Wang, Z., Zhang, T., 2014. Taxonomic relatedness shapes bacterial assembly in activated sludge of globally distributed wastewater treatment plants. Environ. Microbiol. 16(8), 2421-2432.
12. Ju, F., Zhang, T., 2015. Bacterial assembly and temporal dynamics in activated sludge of a full-scale municipal wastewater treatment plant. ISME J. 9(3), 683-696.
13. Kartal, B., Almeida, N.M., Maalcke, W.J., Camp, H.J., Jetten, M.S., Keltjens, J.T., 2013. How to make a living from anaerobic ammonium oxidation. FEMS Microbiol. Rev. 37(3), 428-461.
14. Kim, T.S., Jeong, J.Y., Wells, G.F., Park, H.D., 2013. General and rare bacterial taxa demonstrating different temporal dynamic patterns in an activated sludge bioreactor. Appl. Microbiol. Biotechnol. 97(4), 1755-1765.
15. Kimura, Y., Isaka, K., Kazama, F., 2011. Effects of inorganic carbon limitation on anaerobic ammonium oxidation (anammox) activity. Bioresour. Technol. 102(6), 4390-4394.

16. Lawson, C.E., Strachan, B.J., Hanson, N.W., Hahn, A.S., Hall, E.R., Rabinowitz, B., Mavinic, D.S., Ramey, W.D., Hallam, S.J., 2015. Rare taxa have potential to make metabolic contributions in enhanced biological phosphorus removal ecosystems. Environ. Microbiol. 17(12), 4979-4993.

17. Lawson, C.E., Wu, S., Bhattacharjee, A.S., Hamilton, J.J., McMahon, K.D., Goel, R., Noguera, D.R., 2017. Metabolic network analysis reveals microbial community interactions in anammox granules. Nat. Commun. 8, 15416-15423.

18. Lettinga, G. 2014. *My anaerobic sustainability story*. LeAF Publisher, Wageningen,.

19. Li, J., Qiang, Z., Yu, D., Wang, D., Zhang, P., Li, Y., 2016. Performance and microbial community of simultaneous anammox and denitrification (SAD) process in a sequencing batch reactor. Bioresour. Technol. 218, 1064-1072.

20. Liu, L., Yang, J., Yu, Z., Wilkinson, D.M., 2015. The biogeography of abundant and rare bacterioplankton in the lakes and reservoirs of China. ISME J. 9(9), 2068-77.

21. Luo, J., Chen, H., Han, X., Sun, Y., Yuan, Z., Guo, J., 2017. Microbial community structure and biodiversity of size-fractionated granules in a partial nitritation-anammox process. FEMS Microbiol. Ecol. 93(6).

22. Ma, B., Qian, W., Yuan, C., Yuan, Z., Peng, Y., 2017. Achieving Mainstream Nitrogen Removal through Coupling Anammox with Denitratation. Environ. Sci. Technol. 51(15), 8405-8413.

23. Ma, Y., Sundar, S., Park, H., Chandran, K., 2015. The effect of inorganic carbon on

microbial interactions in a biofilm nitritation-anammox process. Water Res. 70, 246-254.

24. Shu, D., He, Y., Yue, H., Wang, Q., 2016. Metagenomic and quantitative insights into microbial communities and functional genes of nitrogen and iron cycling in twelve wastewater treatment systems. Chem. Eng. J. 290, 21-30.
25. Shu, D., He, Y., Yue, H., Zhu, L., Wang, Q., 2015. Metagenomic insights into the effects of volatile fatty acids on microbial community structures and functional genes in organotrophic anammox process. Bioresour. Technol. 196, 621-633.
26. Strous, M., Kuenen, J.G., Jetten, M.S., 1999. Key physiology of anaerobic ammonium oxidation. Appl Environ Microbiol. 65(7), 3248-3250.
27. van Teeseling, M.C., Mesman, R.J., Kuru, E., Espaillat, A., Cava, F., Brun, Y.V., VanNieuwenhze, M.S., Kartal, B., van Niftrik, L., 2015. Anammox Planctomycetes have a peptidoglycan cell wall. Nat. Commun. 6, 1-10.
28. Winkler, M.K.H., Yang, J., Kleerebezem, R., Plaza, E., Trela, J., Hultman, B., van Loosdrecht, M.C.M., 2012. Nitrate reduction by organotrophic Anammox bacteria in a nitritation/anammox granular sludge and a moving bed biofilm reactor. Bioresour. Technol. 114, 217-223.
29. Wu, W., Logares, R., Huang, B., Hsieh, C.h., 2017. Abundant and rare picoeukaryotic sub- communities present contrasting patterns in the epipelagic waters of marginal seas in the northwestern Pacific Ocean. Environ. Microbiol. 19(1), 287-300.

30. Zhang, F., Peng, Y., Miao, L., Wang, Z., Wang, S., Li, B., 2017. A novel simultaneous partial nitrification Anammox and denitrification (SNAD) with intermittent aeration for cost-effective nitrogen removal from mature landfill leachate. Chem. Eng. J. 313, 619-628.

31. Zhang, X., Yu, B., Zhang, N., Zhang, H., Wang, C., Zhang, H., 2016. Effect of inorganic carbon on nitrogen removal and microbial communities of CANON process in a membrane bioreactor. Bioresour. Technol. 202, 113-8.

32. Zhang, Z., Hu, H., Xu, J., Shi, Z., Shen, Y.a., Shi, M., Jin, R., 2017. Susceptibility, resistance and resilience of anammox biomass to nanoscale copper stress. Bioresour. Technol. 241, 35-43.

33. Zhi, W., Yuan, L., Ji, G., He, C., 2015. Enhanced long-term nitrogen removal and its quantitative molecular mechanism in tidal flow constructed wetlands. Environ. Sci. Technol. 49(7), 4575-4583.

Figure Captions

Fig. 1 The performance of nitrogen removal: (a) the profiles of influent and effluent NH_4^+-N, NO_2^--N, NO_3^--N, and COD concentrations; (b) the profiles of NH_4^+-N, NO_2^--N, and COD removal efficiency; (c) the profiles of NH_4^+-N, NO_2^--N, and NO_3^--N transformation rate; (d) the profiles of nitrogen loading rate (NLR) and nitrogen removal rate (NRR).

Fig. 2 Distribution of phyla in different sub-communities and whole community in different treatment phases. The thickness of each ribbon represents the abundance of each taxon. The absolute tick above the inner segment and relative tick above the outer segment stand for the reads abundances and relative abundance of each taxon, respectively. Others refer to those unclassified reads. The data were visualized using Circos (Version 0.69, http://circos.ca/).

Fig. 3 Network analysis of the genera and operational parameters based on the correlation analysis. Only Spearman's correlation coefficient $\rho > 0.6$ or $\rho < -0.6$) and significant ($q < 0.05$) correlations are shown. Each node represent the relative abundance of genera or nitrogen functional genes. Diamond-shaped nodes represent operational parameters. Solid line represent positive correlations and dash line represent negative correlations. The thickness of each line is proportional to the correlation coefficients of the connections.

Fig. 4 The network analysis revealing the co-occurrence patterns among OTUs. The nodes were colored according to different sub-communities (a) and modularity class (b), respectively. A connection represents a strong (Spearman's correlation coefficient $\rho > 0.6$) and significant ($q < 0.05$) correlation. The size of each node is proportional to the relative abundance of OTUs. The node-level topological features of different sub-communities, namely betweenness (c), closeness (d), transitivity (e), and degree (f). AT, MT, and RT represent abundant taxa, transient taxa, and rare taxa, respectively.

Fig. 5 The functional genes involved in biological nitrogen cycling as predicted by Tax4Fun based on KEGG category (a) and distribution of nitrogen-cycling-related functional genera in different phases according to MiDAS database (b and c). POS and NEG represent positive and negative, respectively.

Fig. 6 Quantitative analysis of nitrogen functional genes in the different phases. Error bars represent standard deviation calculated from three independent experiments.

Fig. 1

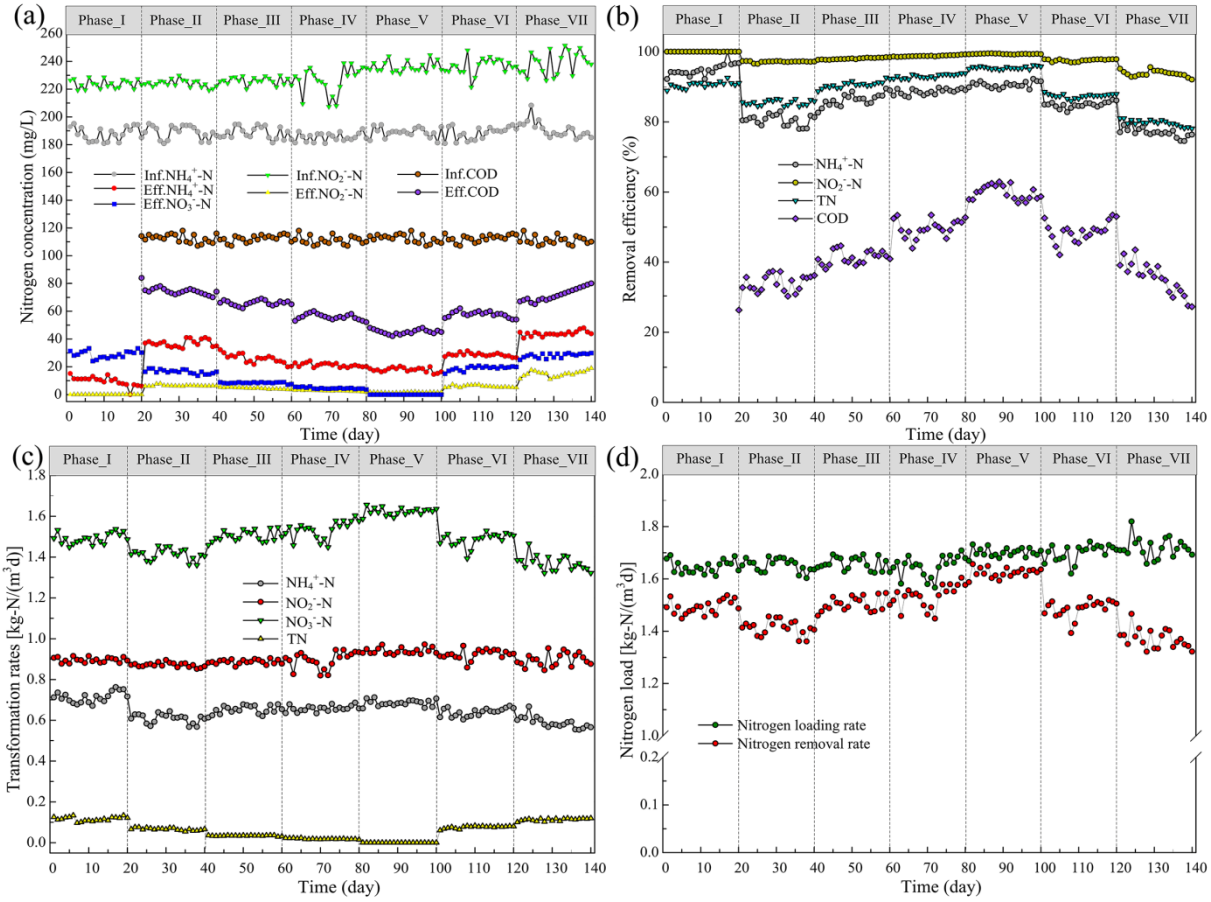

Fig. 1 The performance of nitrogen removal: (a) the profiles of influent and effluent NH_4^+-N, NO_2^--N, NO_3^--N, and COD concentrations; (b) the profiles of NH_4^+-N, NO_2^--N, and COD removal efficiency; (c) the profiles of NH_4^+-N, NO_2^--N, and NO_3^--N transformation rate; (d) the profiles of nitrogen loading rate (NLR) and nitrogen removal rate (NRR).

Fig. 2

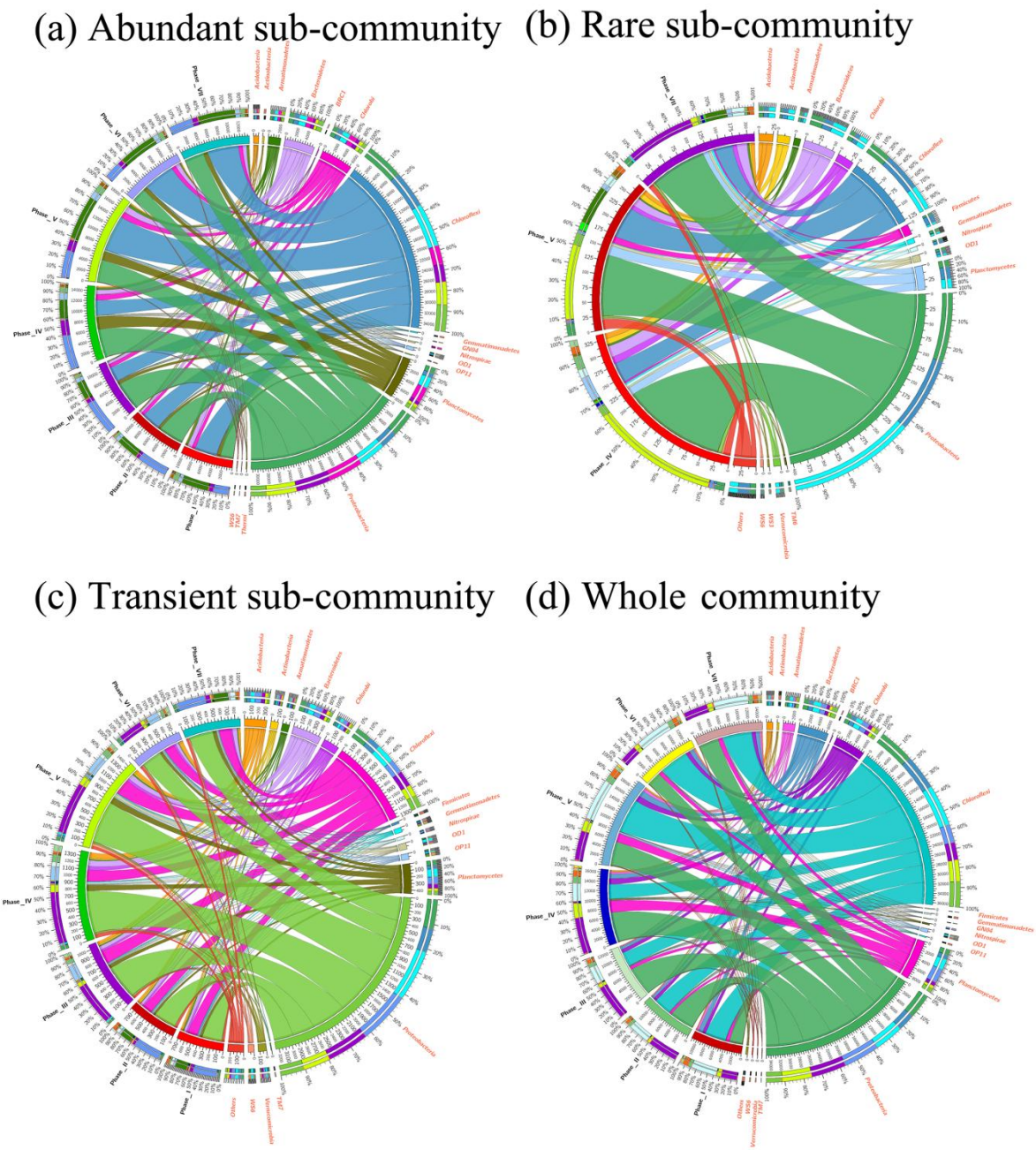

Fig. 2 Distribution of phyla in different sub-communities and whole community in different treatment phases. The thickness of each ribbon represents the abundance of each taxon. The absolute tick above the inner segment and relative tick above the outer segment stand for the reads abundances and relative abundance of each taxon,

respectively. Others refer to those unclassified reads. The data were visualized using Circos (Version 0.69, http://circos.ca/).

Fig. 3

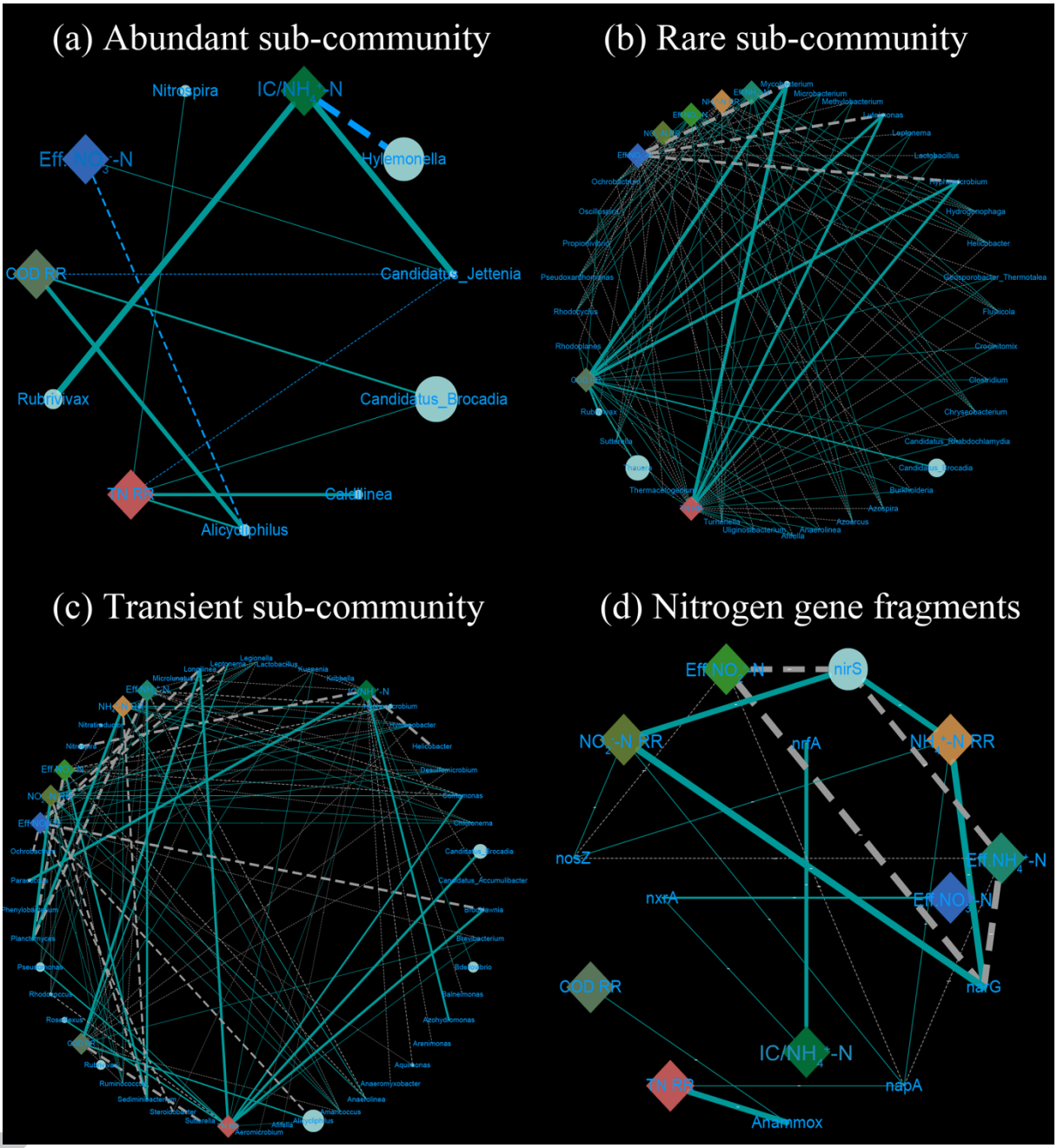

Fig. 3 Network analysis of the genera and operational parameters based on the correlation analysis. Only Spearman's correlation coefficient $\rho > 0.6$ or $\rho < -0.6$) and significant ($q < 0.05$) correlations are shown. Each node represent the relative abundance of genera or nitrogen functional genes. Diamond-shaped nodes represent operational parameters. Solid line represent positive correlations and dash line represent negative

correlations. The thickness of each line is proportional to the correlation coefficients of the connections.

Fig. 4

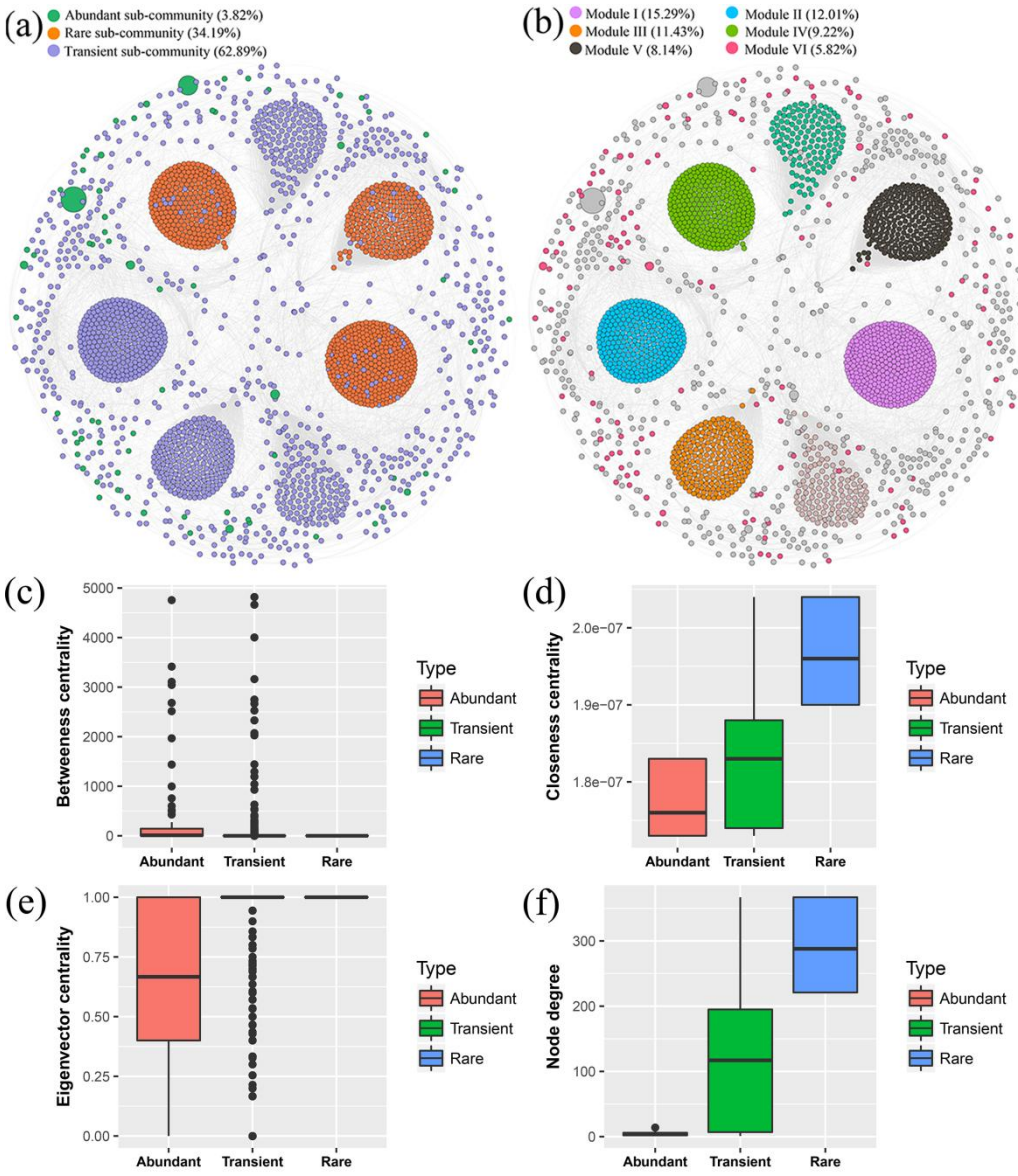

Fig. 4 The network analysis revealing the co-occurrence patterns among OTUs. The nodes were colored according to different sub-communities (a) and modularity class (b), respectively. A connection represents a strong (Spearman's correlation coefficient $\rho > 0.6$) and significant ($q < 0.05$) correlation. The size of each node is proportional to the relative abundance of OTUs. The node-level topological features of different

sub-communities, namely betweenness (c), closeness (d), transitivity (e), and degree (f).

AT, MT, and RT represent abundant taxa, transient taxa, and rare taxa, respectively.

Fig. 5

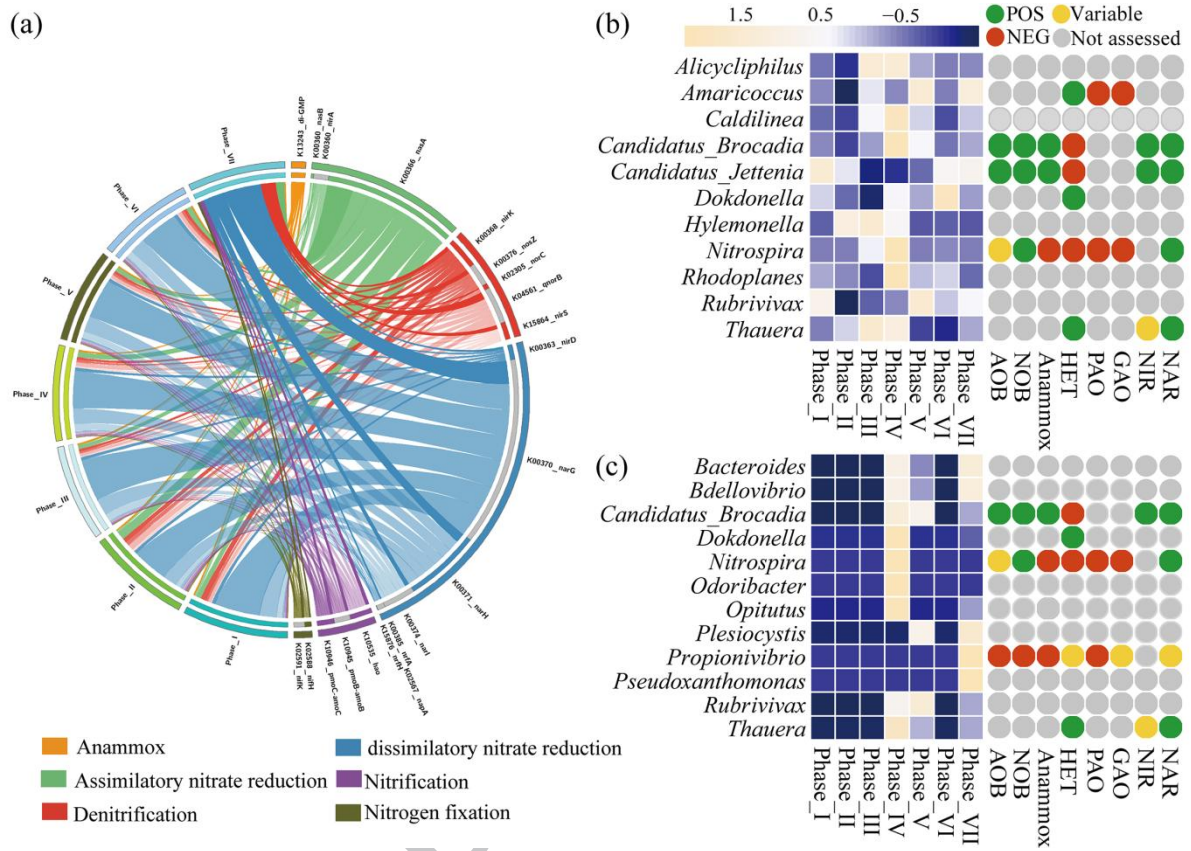

Fig. 5 The functional genes involved in biological nitrogen cycling as predicted by Tax4Fun based on KEGG category (a) and distribution of nitrogen-cycling-related functional genera in different phases according to MiDAS database (b and c). POS and NEG represent positive and negative association, respectively.

Fig. 6

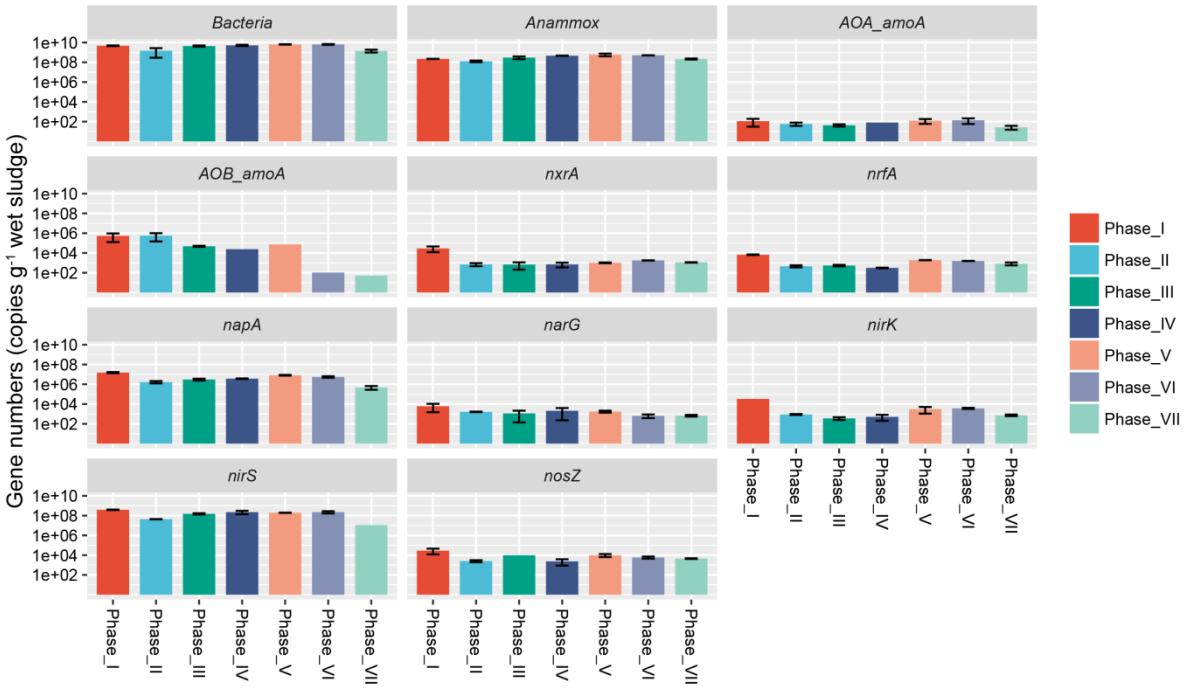

Fig. 6 Quantitative analysis of nitrogen functional genes in the different phases. Error bars represent standard deviation calculated from three independent experiments.

Highlights

- IC/NH_4^+-N ratios have significant influences on NH_4^+-N and TN removal
- Abundant and rare taxa present contrasting patterns under abiotic stresses
- Rare taxa were the key regulators for NH_4^+-N accumulation and NO_2^--N consumption
- Nitrogen removal were mediated by multiple nitrogen transformation pathways

Graphical abstract